International Journal of High-Rise Buildings
June 2021, Vol 10, No 2, 99-107
https://doi.org/10.21022/IJHRB.2021.10.2.99

International Journal of
High-Rise Buildings
www.ctbuh-korea.org/ijhrb/index.php

Performance of Adaptive TMD for Tall Building Damping

Felix Weber[1,†], Fatih Yalniz[2], Deniz Kerner[3], and Peter Huber[4]

[1]*Maurer Switzerland GmbH, 8118 Pfaffhausen, Switzerland*
[2]*Building Structures, WSP USA, New York, NY 10119, USA*
[3]*Maurer SE, 80807 Munich, Germany*
[4]*Maurer SE, 80807 Munich, Germany*

Abstract

This research investigates the potential of Adaptive TMDs for tall building damping. The Adaptive TMD under consideration is based on real-time controlled hydraulic dampers generating purely dissipative control forces. The control approach is designed to enhance the Adaptive TMD efficiency for moderate wind loads with return periods below 50 years. The resulting enhanced TMD efficiency is used to reduce the pendulum mass by 15% compared to the passive TMD while still guaranteeing the acceleration limits of the one and ten year return period winds. Furthermore, the adaptive control approach is designed to disproportionally increase the controlled damping force at wind loads with return periods of 50 years and more in order to reduce the maximum relative motion of the Adaptive TMD with only 85% pendulum mass. Compared to the passive TMD with 100% pendulum mass the maximum relative motion is reduced by 20%. Both the pendulum mass reduction and the maximum relative motion reduction significantly reduce the foot print of the Adaptive TMD which is highly desirable from the economic point of view.

Keywords: Adaptive, Control, Damping, Tall building, TMD, Wind

1. Introduction

One of the reasons for the erection of more and more high-rise buildings is the urbanisation world-wide. High-rise buildings may be susceptible to wind-induced vibrations impeding the vibration comfort of the occupants defined by ISO 10137:2007 for the one year wind and by CTBUH for the ten year wind. The common measure to reduce wind-induced structural accelerations to the acceptable levels is the installation of Tuned Mass Dampers (TMDs) near the top of the building (Tuan and Shang, 2014). There are also other methods that aim at increasing the structural damping by shaping the façade, installation of dampers and energy dissipation devices (Yamashita et al., 2018; Kato et al., 2019; Tsushi et al., 2019; Harada et al., 2020). In some cases tall building may additionally need anti-seismic devices (Tamari et al., 2017; Kim, 2019).

The commonly installed TMD is passive oscillator with damping that, on the one hand, partially compensates for the wind load, and, on the other hand, adds damping to the targeted structural mode (Den Hartog, 1934). Because of this working principle passive TMDs are only efficient within a narrow frequency range in the vicinity of the constant natural frequency of the passive TMD. To increase the efficient frequency bandwidth and – in general – to enhance the vibration reduction efficiency of TMDs actively and semi-actively controlled TMDs have been developed in the past three decades. Active TMDs show the best vibration reduction performance but with the drawback of very high active control forces, increased TMD relative motion and potentially unstable behaviour (Nishimura et al., 1992). A reasonable compromise solution represents semi-active TMDs where the passive oil damper is replaced by a hydraulic damper with real-time controlled bypass valve. The power consumption of the controlled valves including the real-time controller and sensors is very little and the purely dissipative control forces make the semi-active TMD inherently stable. The increased frequency and damping control bandwidth of the semi-active TMD, which is between the fairly narrow bandwidth of the passive TMD and the larger bandwidth of the active TMD, enhances the vibration suppression significantly. The enhanced efficiency can be used to guarantee the same vibration comfort as the passive TMD but with reduced pendulum mass.

This paper presents a special type of semi-active TMD, named Adaptive TMD, that is based on its first development in 2014 for the controlled vibration mitigation of the Danube City Tower (Weber, 2015; Weber et al., 2016), and has been further developed during the last years to make the system more efficient and fail-safe (Weber et al., 2019a and 2019b). The control algorithm is designed to, on the one hand, guarantee the acceleration limits of the one and ten year winds with reduced pendulum mass

[†]Corresponding author: Felix Weber
Tel: +41-44-520-80-69
E-mail: F.Weber@maurer.eu

and, on the other hand, to reduce the maximum TMD relative motion at the maximum 700 year wind. The performance of the Adaptive TMD is demonstrated here for typical building parameters and compared to the results of the optimized passive TMDs with linear and quadratic viscous damping. The performances are assessed in terms of peak structural acceleration, TMD relative motion and hydraulic damper force. The comparative study reveals that the Adaptive TMD is an economical solution for tall building damping because it ensures the acceleration limits for the winds with one and ten year return periods with only 85% of the pendulum mass of the passive TMD and requires less installation space because the maximum TMD relative motion is reduced by 20%.

2. Approach

2.1. Requirements for TMDs in tall buildings

The requirements for TMDs in tall buildings against wind-induced structural vibrations are:

- Guaranteeing the peak structural acceleration limits for the 1 month return period (RP), 6-month RP, 1-year RP, 10-year RP, 50-year RP and 700-year RP winds of which the 1-year RP and 10-year RP acceleration limits are defined by ISO 10137:2007 and CTBUH, respectively.
- Minimizing the TMD space determined by the TMD mass and maximum relative motion due to the maximum wind load (700-year RP).
- TMDs must be failsafe.

Note that TMDs cannot reduce the quasi-static deflection of tall buildings due to the quasi-static wind pressure on the building facade because TMDs can only compensate for dynamic excitation forces.

2.2. Considered TMD types

This comparative study is based on TMD types that are installed in tall buildings (Tuan and Shang, 2014; Weber, 2015; Weber et al., 2016; Weber et al., 2019a and 2019b):

- Passive TMD with linear viscous damping.
- Passive TMD with quadratic viscous damping: This type is commonly installed in tall buildings because the nonlinear damping reduces the maximum TMD relative motion for the 700-year RP wind compared to the passive TMD.
- Adaptive TMD with semi-active hydraulic damper: The actual force of the hydraulic damper is controlled in real-time by the electromagnetically controlled bypass valve. The resulting hydraulic damper force controls in real-time the natural frequency and damping of the pendulum mass (Figure 1). The control system is purely dissipative, i.e. cannot excite the pendulum mass and as such is inherently stable. The frequency and damping controls result in enhanced TMD efficiency which allows guaranteeing the 1-year and 10-year acceleration limits with reduced pendulum mass. At TMD relative motion amplitudes related to the 50-year and 700-year winds the control system produces disproportionally augmented damping to reduce the maximum relative motion of the pendulum mass compared to the classical TMD. The power consumption of the real-time controller, electromagnetic valves, sensors and amplifiers is on the order of 1 to 5 kW. The Adaptive TMD is fail-safe as the valve system of the hydraulic dampers produces passive viscous damping in case of a breakdown of the mains.

TMD types that aim at reducing the installation height by special kinematics, e.g. the compound TMD consisting of a hanging pendulum mass and an inverted pendulum mass or the α-TMD with inclined cables (Weber et al., 2019a), are not additionally considered in this study because these TMD types can be realized either with passive or adaptive hydraulic dampers.

2.3. Goal

This study compares the performance in terms of peak structural acceleration, TMD relative motion and damper force of the optimized Adaptive TMD with reduced pendulum mass with the performances of the optimized passive TMDs with linear and quadratic viscous damping.

2.4. Simulation in modal coordinates

This study is performed by simulation of the building

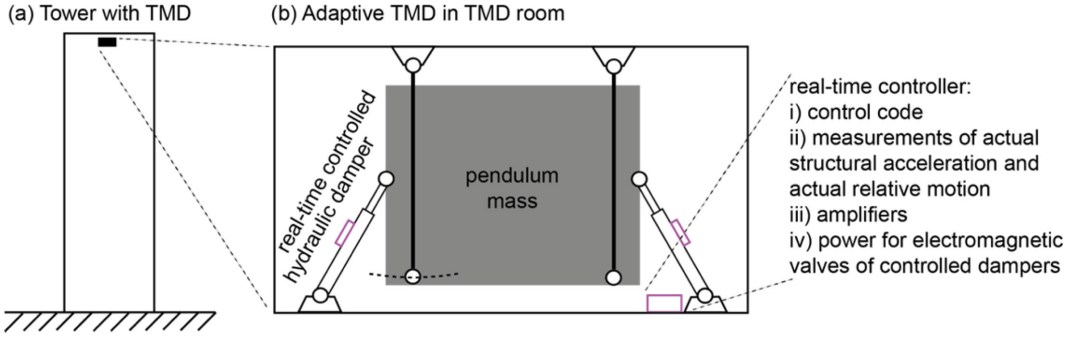


Figure 1. Conceptual sketch of tower with Adaptive TMD: real-time controlled hydraulic dampers control natural frequency and damping of the pendulum mass according to measured structural acceleration and measured relative motion.

with TMD and wind excitation in modal coordinates because TMDs can be tuned to and are efficient in one mode only (Den Hartog, 1934). The wind load in modal coordinates is modelled by a white noise signal that is bandpass filtered such that most excitation energy is in the vicinity of the eigenfrequency of the bending mode to which the TMD is tuned.

2.5. Structural parameters

The energy of the wind load typically shows roll-off behaviour with increasing frequency whereby most wind energy is transferred to the fundamental bending modes of both principal directions. Hence, the fundamental bending modes need to be mitigated by the appropriate designs of the TMD in both principal directions. As the two directions can be assumed as independent the study under consideration is performed for one principal direction. The eigenfrequency f_1 and modal mass m_1, respectively, of the fundamental bending mode of one principal direction are typically in the ranges of 0,12 Hz to 0,18 Hz and 30.000 metric tons to 60.000 metric tons, respectively. To ensure that this study is performed for a typical tower with TMD, the following modal properties are assumed:

- Eigenfrequency $f_1 = 0{,}15$ Hz
- Modal mass $m_1 = 45000$ metric tons
- Damping ratio $\zeta_1 = 1{,}5\%$ (typical assumption for wind-induced vibrations)

2.6. Assessment methods

The simulated time history of the structural acceleration is assessed by the peak acceleration

$$peak\ acceleration = mean(\ddot{x}_1) \pm g_p \sqrt{mean\{(\ddot{x}_1)^2\}} \quad (1)$$

where $\ddot{x}_1$ denotes the acceleration of the considered structural mode and g_p is the peak factor that is derived as follows

$$g_p = \sqrt{2\ln(f_1 T_{\max})} + \frac{0{,}577}{\sqrt{2\ln(f_1 T_{\max})}} \quad (2)$$

where $T_{\max}$ is the simulation time (Huang et al., 2012). The TMD relative motion and the hydraulic damper force are assessed by their extreme values.

2.7. Maximum acceptable peak structural acceleration

For the 1-year RP wind the maximum acceptable peak structural acceleration is defined by ISO 10137:2007 as follows

$$constant\ (f_1)^{-0{,}445} \quad (3)$$

with *constant* = 4,08 for residential buildings and *constant* = 6,12 for office buildings. For the 10-year RP wind the acceptable peak structural acceleration according to CTBUH is 10 to 15 milli-g depending on the use of the building (residential, hotel, office). However, this rather conservative range is often relaxed to 15 to 18 milli-g.

2.8. Optimization of TMDs

The passive TMDs are optimized such that the minimized mass ratio $\mu = m_2/m_1$ guarantees the acceleration limit of the 1-year RP wind for residential buildings (ISO 10137:2007)

$$min\ (\mu)\ for\ peak\ acceleration = 4{,}08\ (f_1)^{-0{,}445} \quad (4)$$

The Adaptive TMD is optimized to comply with ISO 10137:2007 as well but with 85% of the pendulum mass of the regular passive TMD.

3. Modelling

3.1. Passive TMD with linear viscous damping

The equations of motion of the fundamental bending mode with passive TMD with linear viscous damping are described by the following linear differential equation system

$$m_1\ddot{x}_1 + c_1\dot{x}_1 + k_1\dot{x}_1 = f_w - \varphi_2(\varphi_2\dot{x}_1 - \dot{x}_2)c_2 - \varphi_2(\varphi_2 x_1 - x_2)k_2 \quad (5)$$

$$m_2\ddot{x}_2 = (\varphi_2\dot{x}_1 - \dot{x}_2)c_2 + (\varphi_2 x_1 - x_2)k_2 \quad (6)$$

where x_1, $\dot{x}_1$ and $\ddot{x}_1$ denote the displacement, velocity and acceleration of the fundamental bending mode, $k_1 = m_1(2\pi f_1)^2$ and $c_1 = 2\zeta_1 m_1(2\pi f_1)$ are the modal stiffness and viscous damping coefficients, f_w is the wind load in modal coordinates, φ_2 describes the mode shape value at TMD position, x_2, $\dot{x}_2$ and $\ddot{x}_2$ denote the displacement, velocity and acceleration of the TMD mass m_2 relative to ground, $(\varphi_2 x_1 - x_2)$ and $(\varphi_2\dot{x}_1 - \dot{x}_2)$ describe the relative motion and relative velocity of the TMD mass, and k_2 and c_2 are the TMD stiffness and viscous damping coefficients. The mode shape value $\varphi_2 = 0{,}9$ is assumed to account for the facts that the TMD may not placed at the precise mode shape maximum and that small de-tuning effects in k_2 and c_2 due to thermal effects exist. The TMD stiffness $k_2 = m_2(2\pi f_2)^2$ and viscous coefficient $c_2 = 2\zeta_2 m_2(2\pi f_2)$ are defined by the natural TMD frequency f_2 and TMD damping ratio ζ_2 whose optimum values for minimum structural acceleration are given as follows (Asami and Nishihara, 2003)

$$f_2 = \frac{f_1}{\sqrt{1+\mu}} \quad \text{and} \quad \zeta_2 = \sqrt{\frac{3\mu}{4(1+\mu)(2+\mu)}} \quad (7),\ (8)$$

As (7, 8) are valid for $\zeta_1 = 0$ but the study is performed for the realistic case $\zeta_1 = 1{,}5\%$ the TMD viscous coefficient c_2 is numerically optimized by the optimization factor γ

$$c_2 = \gamma\, 2\zeta_2 m_2(2\pi f_2) \quad (9)$$

The optimization of γ for the minimized μ yields

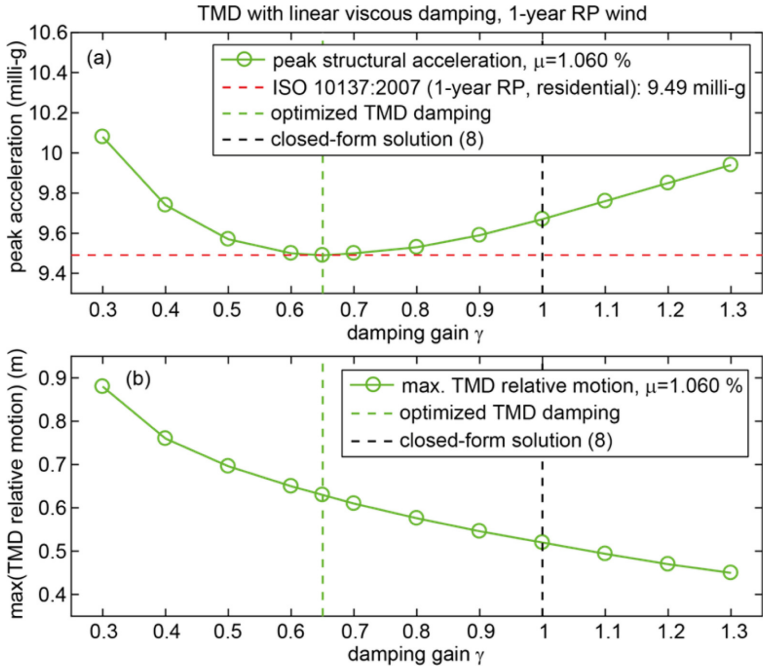


Figure 2. Optimization of mass ratio and damping of TMD with linear viscous damping.

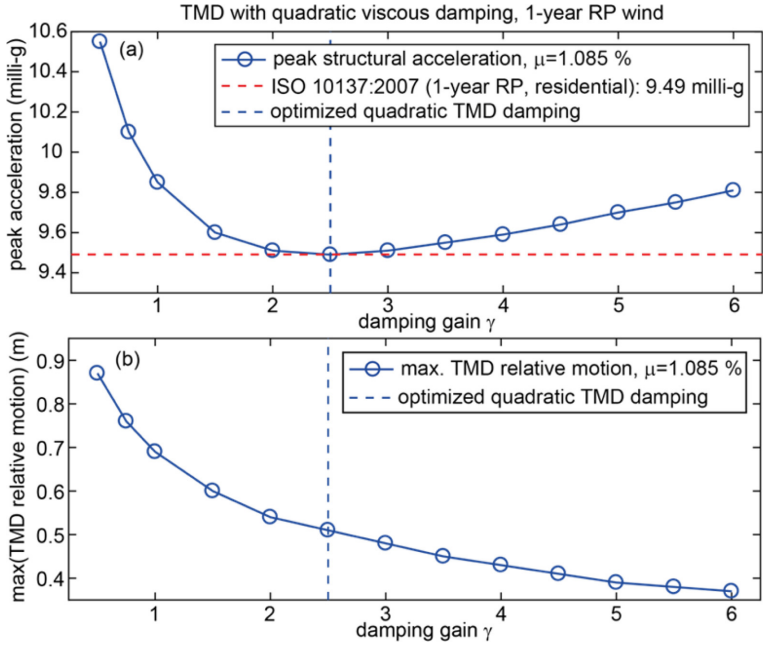


Figure 3. Optimization of mass ratio and damping of TMD with quadratic viscous damping.

$\gamma = 0{,}65$ and $\mu = 1{,}060\%$ for the passive TMD (Figure 2(a)). The optimization demonstrates that optimum TMD damping is not the maximum possible because too high damping would reduce the TMD relative motion and consequently the TMD stiffness force working against the wind load (Figure 2(b)).

3.2. Passive TMD with quadratic viscous damping

The non-linear differential equations of the primary structure with passive TMD with quadratic viscous damping are

$$m_1\ddot{x}_1 + c_1\dot{x}_1 + k_1\dot{x}_1 = f_w - \varphi_2\left(\left|\varphi_2\dot{x}_1 - \dot{x}_2\right|\right)^2 sign(\varphi_2\dot{x}_1 - \dot{x}_2)c_2 - \varphi_2(\varphi_2 x_1 - x_2)k_2 \quad (10)$$

$$m_2\ddot{x}_2 = \left(\left|\varphi_2\dot{x}_1 - \dot{x}_2\right|\right)^2 sign(\varphi_2\dot{x}_1 - \dot{x}_2)c_2 + (\varphi_2 x_1 - x_2)k_2 \quad (11)$$

where *sign* stands for the signum function. Due to the nonlinearity a closed-form solution for the optimum TMD damping does not exist. The optimization of the quadratic viscous damping is made analogue to that of linear viscous damping. The optimum solution $\gamma = 2{,}5$ and $\mu = 1{,}085\%$ points out that the mass ratio of TMDs with quadratic viscous damping must be slightly bigger than that of TMDs with linear viscous damping (Figure 3).

3.3. Adaptive TMD

3.3.1. Equations of motion

The differential equations of the primary structure with Adaptive TMD are as follows

$$m_1\ddot{x}_1 + c_1\dot{x}_1 + k_1\dot{x}_1 = f_w - \varphi_2 f_{sa} - \varphi_2(\varphi_2 x_1 - x_2)k_a \quad (12)$$

$$m_a\ddot{x}_2 = f_{sa} + (\varphi_2 x_1 - x_2)k_a \quad (13)$$

where f_{sa} denotes the force of the semi-actively controlled oil damper, k_a is the stiffness coefficient and m_a the pendulum mass of the Adaptive TMD which is assumed to be 85% of that of the optimized passive TMD with quadratic viscous damping

$$m_a = 0.85 m_2 \quad (14)$$

The stiffness $k_a = m_a(2\pi f_a)^2$ is determined by the natural frequency f_a of the Adaptive TMD that is designed according to the principle of the undamped dynamic vibration absorber (Frahm, 1911)

$$f_a = f_1 \quad (15)$$

3.3.2. Semi-active damper force

The computation of the semi-active force f_{sa} requires several steps. First, the desired control force is computed in real-time based on the measured structural acceleration (accelerometer on the floor of the TMD room) and the measured TMD relative velocity

$$f_{desired,\,active} = -\alpha\ddot{x}_1 + \gamma c_a\left(\left|\varphi_2\dot{x}_1 - \dot{x}_2\right|\right)^2 sign(\varphi_2\dot{x}_1 - \dot{x}_2) \quad (16)$$

where α denotes the feedback gain on structural acceleration. The first term in (16) describes the active control force component, which directly reduces structural accelerations, while the second term controls the TMD relative motion by controlled damping. The viscous coefficient c_a is computed as function of the relative velocity to produce augmented controlled damping at wind loads with RP ≥ 50 years

$$c_a = adaptive\ function(\zeta_2, \gamma, \varphi_2\dot{x}_1 - \dot{x}_2) \quad (17)$$

Since the controlled oil damper exerts dissipative forces only the active forces of (16) must be clipped to zero which yields the desired semi-active control force

$$f_{desired,\,semi\text{-}active} = \begin{cases} f_{desired,active} & : f_{desired,active}(\varphi_2\dot{x}_1 - \dot{x}_2) \geq 0 \\ 0 & : f_{desired,active}(\varphi_2\dot{x}_1 - \dot{x}_2) < 0 \end{cases} \quad (18)$$

The controllable oil damper produces the desired semi-active force (18) if it is within the minimum and maximum quadratic viscous damping forces f_{min} and f_{max} (incl. the negligible small sealing friction of 0,7% of the design force) at fully closed and fully open bypass valve

$$f_{sa} = \begin{cases} f_{\min} & : \left|f_{desired,\,semi-active}\right| < \left|f_{\min}\right| \\ f_{desired,\,semi-active} & : f_{\min} \leq \left|f_{desired,\,semi-active}\right| \leq \left|f_{\max}\right| \\ f_{\max} & : \left|f_{desired,\,semi-active}\right| > \left|f_{\max}\right| \end{cases} \quad (19)$$

3.3.3. Measured prototype and full-scale semi-active damper

Prototype tests of a smaller adaptive hydraulic damper

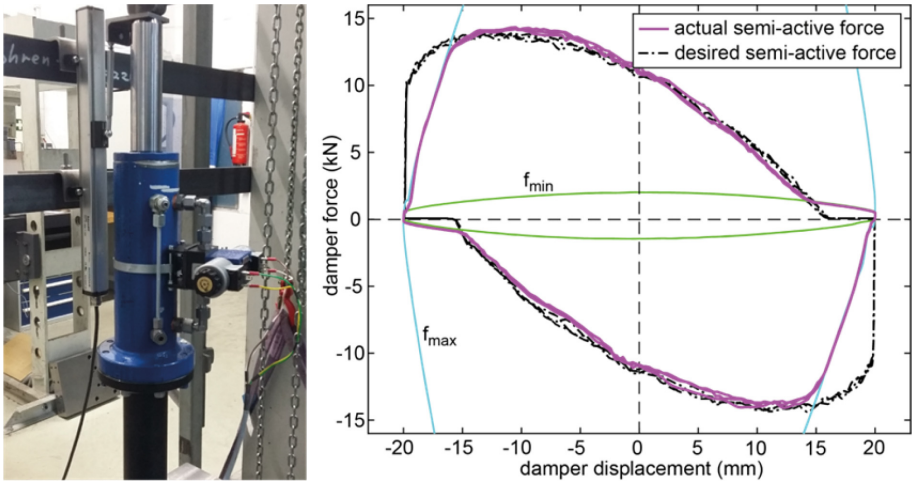


Figure 4. Measured prototype of semi-active damper.

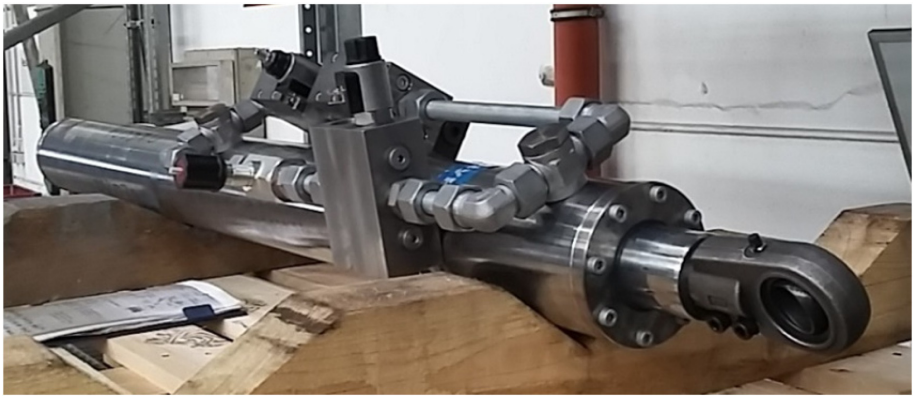


Figure 5. Semi-active damper with design force 100 kN and fail-safe valve system.

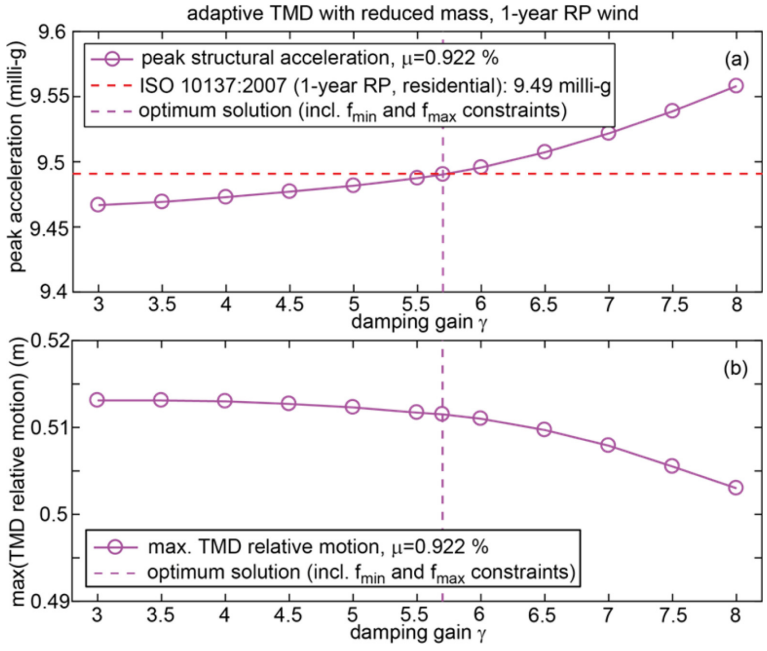


Figure 6. Optimization of damping of Adaptive TMD with reduced mass.

designed for smaller TMD relative motions and greater excitation frequencies are shown in Figure 4. The negative slope of the measured force displacement curve results from the acceleration term in (16). The main control force tracking errors are due to the control force constraints $f_{\min}$ and $f_{\max}$; minor control force tracking errors between $f_{desired,\ active}$ and f_{sa} result from the fact that these tests were made without feedback from a force sensor. Figure 5 depicts the semi-active damper with design force of 100 kN and force feedback. The electro-magnetically controlled bypass valve is enriched with a smart valve system that makes the Adaptive TMD fail-safe. In case of a breakdown of the mains and the back-up batteries at the same time the controlled bypass valve is closed while a passive bypass generating optimum quadratic viscous damping is opened.

3.3.4. Optimization

The Adaptive TMD with 85% of the regular mass is optimized by variation of γ with the consideration of $f_{\min}$ and $f_{\max}$ to guarantee the one year acceleration limit (Figure 6).

4. Results and discussion

The wind load is scaled in amplitude such that the peak structural accelerations without TMD represent typical values of buildings being susceptible to wind-induced vibrations. The same wind load is used to perform the simulations with TMD. The simulation results summarized in Table 1 demonstrate:

- TMDs with optimized linear viscous damping can ensure the acceleration limits but the maximum TMD relative motion resulting from the maximum wind

Table 1. Assessed states depending on wind RP of optimized passive and Adaptive TMDs.

Building	m_2 (t)	Assessed state	Wind return period (year)			
			1	10	50	700
Without TMD	NA	peak accel. (milli-g)	14,00	28,00	42,00	56,00
Passive TMD, optimized linear viscous damping	477,00 (97,7%)	peak accel. (milli-g)	9,49	18,16	25,69	34,61
		TMD rel. motion (m)	0,63	1,19	1,79	2,39
		damper force (kN)	22	40	62	82
Passive TMD, optimized quadratic viscous damping	488,25 (100%)	peak accel. (milli-g)	9,49	18,40	27,01	36,97
		TMD rel. motion (m)	0,51	0,78	0,94	1,11
		damper force (kN)	32	74	113	154
Adaptive TMD, optimized semi-active control	415,01 (85,0%)	peak accel. (milli-g)	9,49	18,11#	27,72	38,93
		TMD rel. motion (m)	0,51	0,77	0,85	0,90*
		damper force (kN)	110	158	226	290

smallest 10-year RP peak structural acceleration
* smallest 700-year RP maximum relative motion

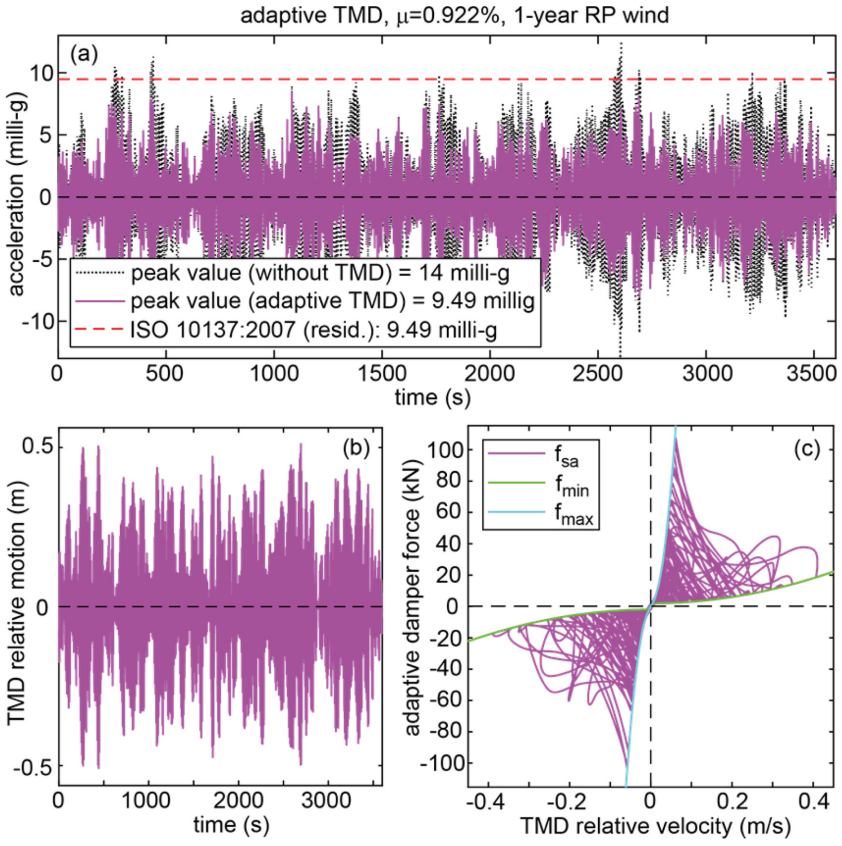


Figure 7. Structural acceleration (a), Adaptive TMD relative motion (b) and adaptive damper force versus relative velocity of Adaptive TMD for 1-year RP wind.

(700-year RP wind) is unacceptably large.

- TMDs with optimized quadratic viscous damping and regular pendulum mass ensure the acceleration limits with acceptable maximum TMD relative motion.
- The presented Adaptive TMD guarantees the acceleration limits for the 1-year and 10-year RP winds with only 85% of the regular pendulum mass thanks to the real-time controls of natural frequency and damping of the pendulum mass and leads to the smallest maximum TMD relative motion (700-year RP) because of the adaptive damping increase at large relative velocities of the pendulum mass related to winds with RP ≥ 50 years (Figure 7). Note that the Adaptive TMD is computed with the consideration of the minimum and

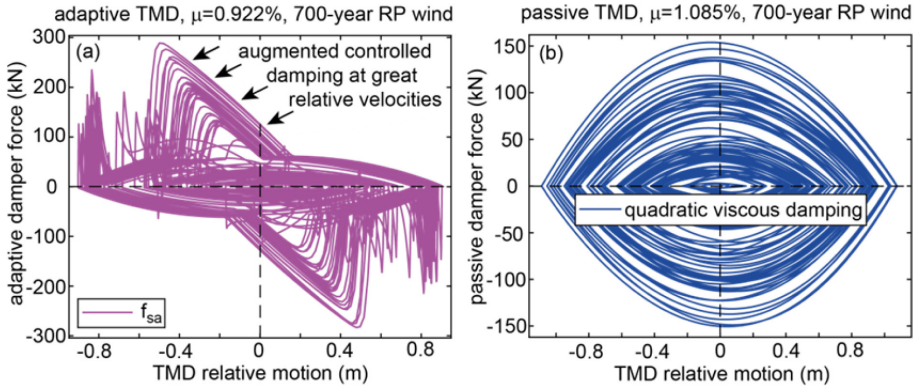


Figure 8. Damper force versus TMD relative motion of (a) Adaptive TMD and (b) passive TMD with quadratic viscous damping for 700-year RP wind.

maximum control force constraints as visible in Figure 7(c). The maximum adaptive damper force is approximately 1,9 times greater than for quadratic viscous damping because of the control force part in proportion to structural acceleration generating the real-time frequency control and because of the augmented adaptive damping at maximum wind loads (Figure 8).

5. Summary and conclusions

The presented Adaptive TMD can guarantee the acceleration limits for the 1-year RP and 10-year RP winds with reduced pendulum mass and – at the same time – leads to reduced maximum relative motion at the maximum considered wind. Both the reduced mass and the reduced relative motion minimize the footprint of the Adaptive TMD which maximizes the building space that can be rented or sold. The additional costs of the real-time control hardware are more than offset by the decreased costs of the smaller pendulum mass and the economic space benefits for the building. In case of a power break down of the mains and the back-up batteries the smart valve system of the controlled hydraulic damper exerts optimum quadratic viscous damping which makes the Adaptive TMD fail-safe. Thus, the presented Adaptive TMD is a highly efficient and robust tool for tall building damping.

Acknowledgements

The authors gratefully acknowledge the support of MAURER SE, Munich, Germany, and Building Structures, WSP USA, New York, USA.

References

Asami, T. and Nishihara, O. (2003). "Closed-Form Exact Solution to Hinf Optimization of Dynamic Vibration Absorbers (Application to Different Transfer Functions and Damping Systems)." *Journal of Vibration and Acoustics, Technical Briefs*, 125, 398-411.

Den Hartog, J. P. (1934). *Mechanical Vibrations.* York, PA: McGraw-Hill Book Company, The Maple Press Company.

Frahm H. (1911). *Devices for damping vibrations of bodies*. US Patent no. 989, 958.

Harada, H., Fukushima, T., and Hatori, T. (2020). "W350 - The Roadmap Of Super High-Rise Timber Building." *International Journal of High-Rise Buildings*, 9(3), 255-260.

Huang, M.-F., Chan, C.-M., Lou, W.-J., and Kwok, K. C.-S. (2012). "Statistical extremes and peak factors in wind-induced vibration of tall buildings." *Journal of Zhejiang University SCIENCE A*, 13, 18-32.

ISO 10137:2007. *Bases for design of structures - Serviceability of buildings and walkways against vibrations*.

Kato, T., Hara, K., and Tanaka, H. (2019). "Structural Design and Construction of High-rise Building to Feature the High-performance Oil Dampers for Vibration Control - Hibiya Mitsui Tower -." *International Journal of High-Rise Buildings*, 8(3), 229-234.

Kim, J. (2019). "Development of Seismic Retrofit Devices for Building Structures." *International Journal of High-Rise Buildings*, 8(3), 221-227.

Nishimura, I., Kobori, T., Sakamoto, M., Koshika, N., Sasaki, K., and Ohrui, S. (1992). "Active tuned mass damper." *Smart Materials and Structures*, 1(4), 306.

Tamari, M., Yoshihara, T., Miyashita, M., Ariyama, N., and Nonoyama, M. (2017). Structural Design and Performance Evaluation of a Mid-story Seismic Isolated High-Rise Building., 6(3), 227-235.

Tsushi, T., Ogura, F., Uekusa, M., Kake, S., Tsuchihashi, T., Yasuda, M., and Furuta, T. (2019). "Structural Design of High-Rise Concrete Condominium With Wall Dampers for Vibration Control." *International Journal of High-Rise Buildings*, 8(3), 201-209.

Tuan, A. Y. and Shang, G. Q. (2014). "Vibration Control in a 101-Storey Building Using a Tuned Mass Damper." *Journal of Applied Science and Engineering*, 17(2), 141-156.

Weber, F. (2015). "Robust force tracking control scheme for MR dampers." *Struct. Control Health Monit.*, 22(12), 1373-1395.

Weber, F., Huber, P., Distl, H., and Braun, C. (2016). "Real-time controlled TMD of Danube City Tower." *Proceeding of the CTBUH (Council on Tall Buildings and Urban Habitat) International Conference 2016*, Shenzhen, Guangzhou, Hong Kong (China), 16-21 October 2016.

Weber, F., Huber, P., Spensberger, S., Okumusoglu, D., Distl, J., and Braun, C. (2019a). "Adaptive TMD System for Reduced Space Demand in Tall Buildings." *Proceedings of the IABSE Symposium New York 2019*, New York, USA.

Weber, F., Huber, P., Spensberger, S., Distl, J., and Braun, C. (2019b). "Reduced-mass Adaptive TMD for Tall Buildings Damping." *International Journal of High-Rise Buildings*, 8(2), 117-123.

Yamashita, Y., Kushima, S., Okuno, Y., and Morishita, T. (2018). "Structural Design and Construction for Tall Damped Building with Irregularly-Shaped Plan and Elevation." *International Journal of High-Rise Buildings*, 7(3), 255-264.